Ukrainian Journal of Physical Optics
ISSUE 3
2024

BIFURCATION ANALYSIS AND OPTICAL SOLITONS FOR THE DISPERSIVE CONCATENATION MODEL

LU TANG[1], YAKUP YILDIRIM[2,3], ANWAR JAAFAR MOHAMAD JAWAD[4], ANJAN BISWAS[5,6,7,8] & ALI SALEH ALSHOMRANI[6]

[1]School of Mathematics and Physics, Chengdu University of Technology, Chengdu–610059, China
[2]Department of Computer Engineering, Biruni University, Istanbul–34010, Turkey
[3]Department of Mathematics, Near East University, 99138 Nicosia, Cyprus
[4]Department of Computer Technical Engineering, Al Rafidain University College, 10064 Baghdad, Iraq
[5]Department of Mathematics and Physics, Grambling State University, Grambling, LA 71245–2715, USA
[6]Mathematical Modeling and Applied Computation (MMAC) Research Group, Center of Modern Mathematical Sciences and their Applications (CMMSA), Department of Mathematics, King Abdulaziz University, Jeddah–21589, Saudi Arabia
[7]Department of Applied Sciences, Cross–Border Faculty of Humanities, Economics and Engineering, University of Galati, 111 Domneasca Street, Galati—800201, Romania
[8]Department of Mathematics and Applied Mathematics, Sefako Makgatho Health Sciences University, Medunsa–0204, South Africa

Received: 04.12.2023

Abstract. This work carries out the bifurcation analysis of the dispersive concatenation model with Kerr law of self-phase modulation. The dynamical system is first formulated and the phase-plane portraits are analyzed. The corresponding soliton solutins are subsequently recovered from the analysis.

Keywords: bifurcation analysis, optical solitons, dispersive concatenation model
UDC: 535.32
DOI: doi: 10.3116/16091833/Ukr.J.Phys.Opt.2024.03031

1. Introduction

The study of optical solitons has been going on for the past few decades, and this area of research in nonlinear optics is still burning bright [1-20]. One of the several models that have been addressed is the dispersive concatenation model. It is a sequel to the concatenation model first proposed in 2014 [8, 9]. Subsequently, the same group proposed its dispersive version the following year. This form of the concatenation model contains higher-order dispersion terms and is, therefore, referred to as the dispersive concatenation model. It conjoins three of the familiar models from nonlinear optics that governs the propagation of solitons through optical fibers across trans-continental and trans-oceanic distances. These are the Schrodinger-Hirota equation (SHE), the Lakshmanan-Porsezian-Daniel (LPD) model, and the dispersive nonlinear Schrodinger's equation (NLSE).

The model has been extensively studied during the past year using several approaches. The conservation laws have been retrieved [21], the model was next studied with a power-law form of self-phase modulation (SPM) [22], the quiescent optical solitons have been recovered for the model with nonlinear chromatic dispersion [23], the method of undetermined coefficients was applied to gain a full spectrum of optical solitons [24], and the conservation laws for the model with power-law of SPM were also reported [25, 26]. The current paper turns the page to address the bifurcation analysis of the model. The corresponding dynamical system is analyzed, and the phase portraits are exhibited for the model. Subsequently, using this approach, the cnoidal waves

and the soliton solutions are retrieved for the model.

It must be noted that bifurcation analysis for the Radhakrishnan-Kundu-Lakshmanan (RKL) equation has already been studied in the past [21]. For the RKL model, the bifurcation analysis led to the formulation of dispersive optical solitons. However, the current model, which is the dispersive concatenation model, involves the conjunction of three well-known models containing third-order dispersion (3OD), fourth-order dispersion, as well as fifth-order dispersive effects stemming from the SHE, LPD model, and the dispersive NLSE. This is a departure from the RKL equation, which contains only 3OD. The current model addressed in this paper, with higher-order dispersion terms and a conjunction of three well-known models, may lead to new results.

2. Mathematical analysis and phase portraits

In the current work, the concatenation model in its dimensionless form is considered in the following form

$$\begin{aligned} &iu_t + a_1 u_{xx} + b_1 |u|^2 u - i\alpha_1 \left(\delta_1 u_{xxx} + \delta_2 |u|^2 u_x\right) \\ &+\alpha_2 \left(\delta_3 u_{xxxx} + \delta_4 |u|^2 u_{xx} + \delta_5 |u|^4 u + \delta_6 |u_x|^2 u + \delta_7 u_x^2 u^* + \delta_8 u^2 u_{xx}^*\right) \\ &-i\alpha_3 \left(\delta_9 u_{xxxxx} + \delta_{10} |u|^2 u_{xxx} + \delta_{11} |u|^4 u_x + \delta_{12} u u_x u_{xx}^*\right. \\ &\left.+\delta_{13} u^* u_x u_{xx} + \delta_{14} u u_x^* u_{xx} + \delta_{15} u_x^* u_x^2\right) = 0, \end{aligned} \tag{1}$$

where $u = u(x,t)$ is the complex-valued wave function, which represents the soliton profile. x denotes the normalized propagation and t stands for the retard time. The first five terms are from SHE, while the coefficient of α_2 is from the LPD equation, and the coefficient of α_3 is from the dispersive NLSE. The coefficient of a_1 is the chromatic dispersion while the coefficient of b_1 accounts for the Kerr law of SPM. Finally, the coefficients of δ_j for j = 1,....,15 and α_j for j = 1, 2, 3 are all real-valued constants. x denotes the normalized propagation and t stands for the retard time. The first five terms are from SHE while coefficient of α_2 are from the LPD equation and the coeffocient of α_3 are from the dispersive NLSE. The coefficient of a_1 is the chromatic dispersion while the coefficient of b_1 accounts for the Kerr law of SPM. Finally, the coefficients of δ_j for j = 1,....,15 and α_j for j = 1, 2, 3 are all real-valued constants.

In order to derive optical soliton solutions, traveling wave solutions, and bifurcation phase diagrams for the concatenation model (1), we first decompose:

$$u(x,t) = \Phi(\xi) e^{i\eta(x,t)}, \; \xi = k(x - v_0 t), \; \eta(x,t) = -\lambda x + \mu t + \theta_0, \tag{2}$$

where $\Phi(\xi)$ is a real-valued function representing the amplitude component of the soliton, and v_0 represents its velocity. The coefficient μ represents the frequency of soliton, while λ and θ_0 denote the wave number and phase constant, respectively. Substituting (2) into (1) and then decomposing it into real and imaginary parts, we get:

Real part:

$$\begin{aligned} &\left(a_1\lambda^2 + \alpha_3\lambda^5\delta_9 - \alpha_2\lambda^4\delta_3 - \alpha_1\lambda^3\delta_1 + \mu\right)\Phi - k^2\left(a_1 + 10\alpha_3\lambda^3\delta_9 - 6\alpha_2\lambda^2\delta_3 - 3\alpha_1\lambda\delta_1\right)\Phi'' \\ &+\left[-\alpha_3\lambda^3\delta_{10} - \alpha_3\lambda^3\delta_{12} - \alpha_3\lambda^3\delta_{13} + \alpha_3\lambda^3\delta_{14} + \alpha_3\lambda^3\delta_{15}\right. \\ &\left.+\alpha_2\lambda^2\left(\delta_4 + \delta_6 + \delta_7 + \delta_8\right) + \alpha_1\lambda\delta_2 - b_1\right]\Phi^3 \\ &+k^2\left[\alpha_3\lambda\left(-2\delta_{12} + 2\delta_{13} + 2\delta_{14} + \delta_{15}\right) - \alpha_2\left(\delta_6 + \delta_7\right)\right]\Phi\Phi'^2 + \left(\alpha_3\lambda\delta_{11} - \alpha_2\delta_5\right)\Phi^5 \\ &+k^2\left[\alpha_3\lambda\left(3\delta_{10} + \delta_{12} + \delta_{13} - \delta_{14}\right) - \alpha_2\left(\delta_4 + \delta_8\right)\right]\Phi^2\Phi'' + k^4\left(5\alpha_3\lambda\delta_9 - \alpha_2\delta_3\right)\Phi'''' = 0. \end{aligned} \tag{3}$$

Imaginary part:

$$\begin{aligned}&(2a_1\lambda+5\alpha_3\lambda^4\delta_9-4\alpha_2\lambda^3\delta_3-3\alpha_1\lambda^2\delta_1+v_0)\Phi'+\alpha_3k^3\delta_{15}\Phi'^3+\alpha_3k\delta_{11}\Phi^4\Phi'\\&+k[\lambda(\alpha_3\lambda(-3\delta_{10}+\delta_{12}-3\delta_{13}+\delta_{14}+\delta_{15})+2\alpha_2(\delta_4+\delta_6+\delta_7-\delta_8))+\alpha_1\delta_2]\Phi^2\Phi'\\&+k^3(4\alpha_2\lambda\delta_3+\alpha_1\delta_1-10\alpha_3\lambda^2\delta_9)\Phi'''+\alpha_3k^3(\delta_{12}+\delta_{13}+\delta_{14})\Phi\Phi'\Phi''\\&+\alpha_3k^3\delta_{10}\Phi^2\Phi'''+\alpha_3k^5\delta_9\Phi^2\Phi''''=0.\end{aligned}\tag{4}$$

Certain restrictions are provided by Eq. (3) when the coefficients of its linearly independent functions are set to zero, as shown below

$$a_1\lambda^2+\alpha_3\lambda^5\delta_9-\alpha_2\lambda^4\delta_3-\alpha_1\lambda^3\delta_1+\mu=0,\tag{5}$$

$$-k^2\left(a_1+10\alpha_3\lambda^3\delta_9-6\alpha_2\lambda^2\delta_3-3\alpha_1\lambda\delta_1\right)=0,\tag{6}$$

$$\begin{aligned}&-\alpha_3\lambda^3\delta_{10}-\alpha_3\lambda^3\delta_{12}-\alpha_3\lambda^3\delta_{13}+\alpha_3\lambda^3\delta_{14}+\alpha_3\lambda^3\delta_{15}\\&+\alpha_2\lambda^2\left(\delta_4+\delta_6+\delta_7+\delta_8\right)+\alpha_1\lambda\delta_2-b_1=0,\end{aligned}\tag{7}$$

$$k^2\left[\alpha_3\lambda\left(-2\delta_{12}+2\delta_{13}+2\delta_{14}+\delta_{15}\right)-\alpha_2\left(\delta_6+\delta_7\right)\right]=0,\tag{8}$$

$$\alpha_3\lambda\delta_{11}-\alpha_2\delta_5=0,\tag{9}$$

$$k^2\left[\alpha_3\lambda\left(3\delta_{10}+\delta_{12}+\delta_{13}-\delta_{14}\right)-\alpha_2\left(\delta_4+\delta_8\right)\right]=0,\tag{10}$$

and

$$k^4\left(5\alpha_3\lambda\delta_9-\alpha_2\delta_3\right)=0.\tag{11}$$

According to the imaginary part (4), we know that the soliton speed reaches:

$$v_0=-2a_1\lambda+4\alpha_2\lambda^3\delta_3+3\alpha_1\lambda^2\delta_1,\tag{12}$$

along with the parameter constraints:

$$\lambda\left(2\alpha_2\left(\delta_4+\delta_6+\delta_7-\delta_8\right)-4\alpha_3\lambda\delta_{13}\right)+\alpha_1\delta_2=0,\tag{13}$$

$$\delta_9=\delta_{10}=\delta_{11}=\delta_{15}=0,\tag{14}$$

$$\delta_{12}+\delta_{13}+\delta_{14}=0,\tag{15}$$

and

$$4\alpha_2\lambda\delta_3+\alpha_1\delta_1=0.\tag{16}$$

From the restrictions (14)-(16), Eq. (4) can be rewritten as follows:

$$\begin{aligned}&k^2(4\alpha_2\lambda\delta_3+\alpha_1\delta_1)\Phi'''+(2a_1\lambda+\lambda^2\alpha_1\delta_1-3\alpha_1\lambda^2\delta_1+v_0)\Phi'\\&+[\lambda(-4\alpha_3\lambda\delta_{13}+2\alpha_2(\delta_4+\delta_6+\delta_7-\delta_8))+\alpha_1\delta_2]\Phi^2\Phi'=0.\end{aligned}\tag{17}$$

Integrating Eq. (17) once, one has

$$\begin{aligned}\Phi''=&-\frac{-4\alpha_3\lambda^2\delta_{13}+2\lambda\alpha_2\left(\delta_4+\delta_6+\delta_7-\delta_8\right)+\alpha_1\delta_2}{3k^2\left(4\alpha_2\lambda\delta_3+\alpha_1\delta_1\right)}\Phi^3\\&-\frac{2a_1\lambda+\lambda^2\alpha_1\delta_1-3\alpha_1\lambda^2\delta_1+v_0}{k^2\left(4\alpha_2\lambda\delta_3+\alpha_1\delta_1\right)}\Phi.\end{aligned}\tag{18}$$

For Eq. (18), denote $\Phi'=y$, it is easy to find that Eq. (18) can be transformed as the following planar dynamical system

$$\begin{cases}\dfrac{d\Phi}{d\xi}=y,\\[2ex]\dfrac{dy}{d\xi}=-N_{1h}\Phi^3+N_{2h}\Phi,\end{cases}\tag{19}$$

with the Hamiltonian system

$$H(\Phi, y) = \frac{1}{2}y^2 + \frac{N_{1h}}{4}\Phi^4 - \frac{N_{2h}}{2}\Phi^2 = h, \tag{20}$$

where

$$N_{1h} = \frac{-4\alpha_3\lambda^2\delta_{13} + 2\lambda\alpha_2(\delta_4 + \delta_6 + \delta_7 - \delta_8) + \alpha_1\delta_2}{3k^2(4\alpha_2\lambda\delta_3 + \alpha_1\delta_1)},$$

and

$$N_{2h} = -\frac{2a_1\lambda + \lambda^2\alpha_1\delta_1 - 3\alpha_1\lambda^2\delta_1 + v_0}{k^2(4\alpha_2\lambda\delta_3 + \alpha_1\delta_1)}.$$

Note $H(\Phi) = -N_{1h}\Phi^3 + N_{2h}\Phi$. When $N_{1h}N_{2h} > 0$, we obtain there exist three zeros of $H(\Phi)$, which include $\Phi_0 = 0$, $\Phi_1 = -\sqrt{\frac{N_{2h}}{N_{1h}}}$ and $\Phi_2 = \sqrt{\frac{N_{2h}}{N_{1h}}}$. When $N_{1h}N_{2h} < 0$, we get one zero of $H(\Phi)$, which is $\Phi_3 = 0$. Assume that $S_i(\Phi_i, 0)$ $(i = 0, 1, 2)$ represents the equilibrium points of the system (19). Thus, the eigenvalue of (19) at the equilibrium point is $\lambda_{1,2} = \pm\sqrt{H'(\Phi)}$. It follows from the bifurcation theory of planar dynamical systems [3, 4], we obtain that the point $S_i(\Phi_i, 0)$ is called saddle point if $H'(\Phi_i) > 0$. The point $S_i(\Phi_i, 0)$ is called a degraded point if $H'(\Phi_i) = 0$. The point $S_i(\Phi_i, 0)$ is called the center point if $H'(\Phi_i) < 0$. From this, we get the phase portraits of the system (19) that depend on different parameters N_{1h} and N_{2h}, shown in Fig. 1 and Fig. 2.

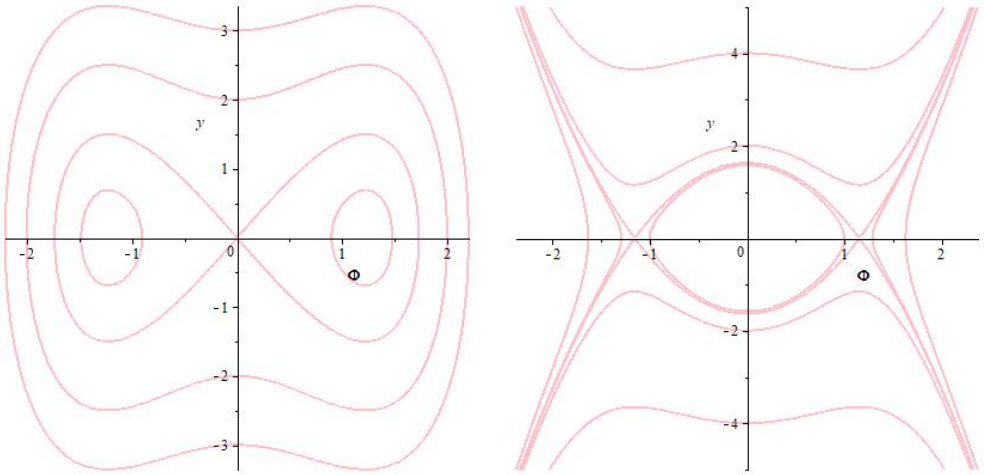

(a) (b)

Fig. 1. The bifurcation phase portraits of the system (19): (a) the case $N_{1h} > 0$, $N_{2h} > 0$; (b) the case $N_{1h} < 0$, $N_{2h} < 0$.

Case 1. $N_{1h} > 0$, $N_{2h} > 0$.

In this case, it is notable that $S_1\left(-\sqrt{N_{2h}/N_{1h}}, 0\right)$ and $S_2\left(\sqrt{N_{2h}/N_{1h}}, 0\right)$ stand for the center points, while the origin point $S_0(0,0)$ represents a saddle point.

(i) For $h \in \left(-N_{2h}^2/4N_{1h}, 0\right)$, we find two families of periodic orbits (see Fig. 1(a)). Thus the Eq. (19) can be rewritten as follows:

$$y^2=\frac{N_{1h}}{2}\left(-\Phi^4+\frac{2N_{2h}}{N_{1h}}\Phi^2+\frac{4h}{N_{1h}}\right)=\frac{N_{1h}}{2}\left(\Phi^2-\phi_{1m}^2\right)\left(\phi_{2m}^2-\Phi^2\right), \tag{21}$$

where $\phi_{1m}^2=\frac{N_{2h}}{N_{1h}}-\frac{1}{N_{1h}}\sqrt{N_{2h}^2+4N_{1h}h}$, and $\phi_{2m}^2=\frac{N_{2h}}{N_{1h}}+\frac{1}{N_{1h}}\sqrt{N_{2h}^2+4N_{1h}h}$.

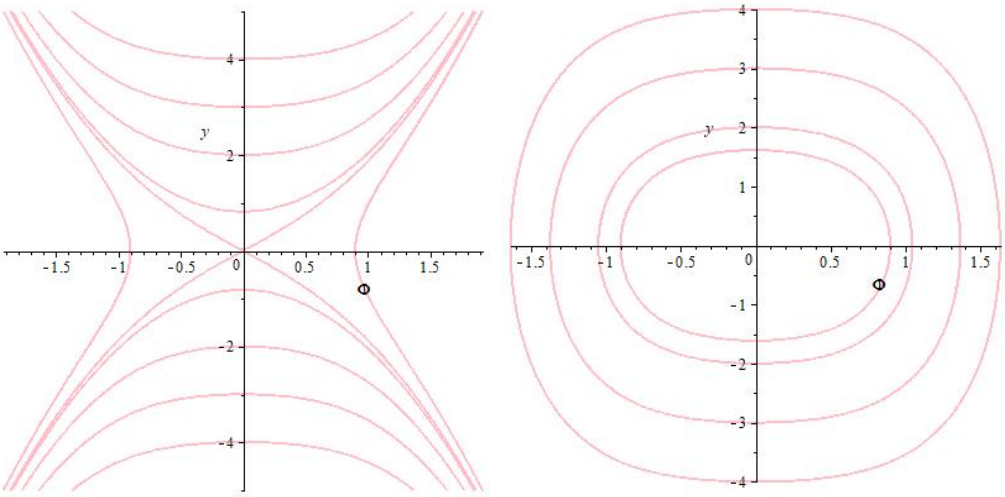

(a) (b)

Fig. 2. The bifurcation phase portraits of the system (19): (a) the case $N_{1h}<0$, $N_{2h}>0$; (b) the case $N_{1h}>0$, $N_{2h}<0$.

By integrating the first equation of Eq. (19) along the periodic orbits in the right(left) half-plane via the Eq. (20), one has

$$\int_{\Phi}^{\phi_{2m}}\frac{dy}{\sqrt{\left(y^2-\phi_{1m}^2\right)\left(\phi_{2m}^2-y^2\right)}}=\mp\sqrt{\frac{N_{1h}}{2}}\left(\xi-\xi_0\right), \tag{22}$$

and

$$\int_{-\phi_{2m}}^{\Phi}\frac{dy}{\sqrt{\left(y^2-\phi_{1m}^2\right)\left(\phi_{2m}^2-y^2\right)}}=\pm\sqrt{\frac{N_{1h}}{2}}\left(\xi-\xi_0\right). \tag{23}$$

From the Eqs. (2), (22), and (23), the smooth periodic wave solutions of system (1) take the form

$$u_1(x,t)=\pm\phi_{2m}\mathrm{dn}\left(\phi_{2m}\sqrt{\frac{N_{1h}}{2}}\left(k\left(x-v_0t\right)-\xi_0\right),\frac{\sqrt{\phi_{2m}^2-\phi_{1m}^2}}{\phi_{2m}}\right)\exp\left(i\left(-\lambda x+\mu t+\theta_0\right)\right), \tag{24}$$

where $\mathrm{dn}(*,*)$ is the Jacobi elliptic function.

(ii) For $h=0$, we find that $\phi_{1m}^2=0$ and $\phi_{2m}^2=2N_{2h}/N_{1h}$. As a result, we construct two families of bell-shaped soliton solutions of Eq. (1) in the following form (see Fig. 3):

$$u_2(x,t)=\pm\sqrt{\frac{2N_{2h}}{N_{1h}}}\mathrm{sech}\left(\sqrt{N_{2h}}\left(k\left(x-v_0t\right)-\xi_0\right)\right)\times\exp\left(i\left(-\lambda x+\mu t+\theta_0\right)\right). \tag{25}$$

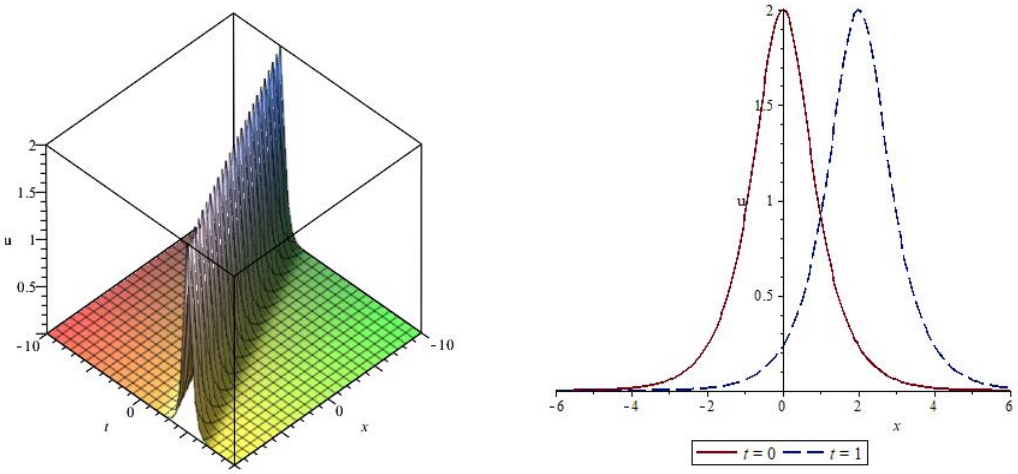

(a) (b)

Fig. 3. The graphics of bell-shaped soliton solution given by Eq. (25) at $N_{1h}=1$, $N_{2h}=2$, $v_0=2$, $k=1$, and $\xi_0=0$: (a) real 3D surface; (b) real 2D surface.

(iii) For $h\in(0,+\infty)$, the first equation of Eq. (19) can be rewritten as follows:

$$y^2=\frac{N_{1h}}{2}\left(-\Phi^4+\frac{2N_{2h}}{N_{1h}}\Phi^2+\frac{4h}{N_{1h}}\right)=\frac{N_{1h}}{2}\left(\Phi^2+\phi_{3m}^2\right)\left(\phi_{4m}^2-\Phi^2\right), \tag{26}$$

where

$$\phi_{3m}^2=-\frac{N_{2h}}{N_{1h}}+\frac{1}{N_{1h}}\sqrt{N_{2h}^2+4N_{1h}h}\,,$$

and

$$\phi_{4m}^2=\frac{N_{2h}}{N_{1h}}+\frac{1}{N_{1h}}\sqrt{N_{2h}^2+4N_{1h}h}\,.$$

Next integrating the first equation of system (19) along the periodic orbits in the right(left) half-plane via Eq. (26), one has:

$$\int_0^{\Phi}\frac{dy}{\sqrt{\left(y^2+\phi_{3m}^2\right)\left(\phi_{4m}^2-y^2\right)}}=\pm\sqrt{\frac{N_{1h}}{2}}\left(\xi-\xi_0\right). \tag{27}$$

It follows from Eqs. (2) and (27), we derive two families of periodic soliton solutions of system (1) that take the form:

$$u_3(x,t)=\pm\phi_{4m}\mathrm{cn}\left(\sqrt{\frac{N_{1h}\left(\phi_{3m}^2+\phi_{4m}^2\right)}{2}}\left(k\left(x-v_0t\right)-\xi_0\right),\frac{\phi_{4m}}{\sqrt{\phi_{3m}^2+\phi_{4m}^2}}\right), \tag{28}$$
$$\times\exp\left(i\left(-\lambda x+\mu t+\theta_0\right)\right)$$

where $\mathrm{cn}(*,*)$ is the Jacobi elliptic function.

Case 2. $N_{1h}<0$, $N_{2h}<0$.

Under the conditions of $N_{1h}<0$, and $N_{2h}<0$, it is notable that the system (19) has two heteroclinic orbits, which connect two saddle points $S_1\left(-\sqrt{N_{2h}/N_{1h}},0\right)$ and $S_2\left(\sqrt{N_{2h}/N_{1h}},0\right)$. Thus, there is a family periodic orbits, which enclose center point $S_0(0,0)$ (see Fig. 1(b)).

(i) For $h\in\left(0,-\frac{N_{2h}^2}{4N_{1h}}\right)$, we deduce a family of periodic of (19) defined by the algebraic equation as follows:

$$y^2=-\frac{N_{1h}}{2}\left(\Phi^4+\frac{2N_{2h}}{N_{1h}}\Phi^2-\frac{4h}{N_{1h}}\right)=-\frac{N_{1h}}{2}\left(\phi_{5m}^2-\Phi^2\right)\left(\phi_{6m}^2-\Phi^2\right), \tag{29}$$

where $\phi_{5m}^2=\frac{N_{2h}}{N_{1h}}-\frac{1}{N_{1h}}\sqrt{N_{2h}^2+4N_{1h}h}$, and $\phi_{6m}^2=\frac{N_{2h}}{N_{1h}}+\frac{1}{N_{1h}}\sqrt{N_{2h}^2+4N_{1h}h}$.

Substituting Eq. (29) into the first equation of (19) and integrating them along the periodic orbits, one has:

$$\int_0^{\Phi}\frac{dy}{\sqrt{\left(\phi_{5m}^2-y^2\right)\left(\phi_{6m}^2-y^2\right)}}=\pm\sqrt{-\frac{N_{1h}}{2}}\left(\xi-\xi_0\right). \tag{30}$$

From Eqs. (2) and (30), the periodic soliton solutions of system (1) take the form:

$$u_4(x,t)=\pm\phi_{5m}\mathrm{sn}\left(\phi_{6m}\sqrt{-\frac{N_{1h}}{2}}\left(k\left(x-v_0t\right)-\xi_0\right),\frac{\phi_{5m}}{\phi_{6m}}\right)\times\exp\left(i\left(-\lambda x+\mu t+\theta_0\right)\right), \tag{31}$$

where $\mathrm{sn}(*,*)$ is the Jacobi elliptic function.

(ii) For $h=-\frac{N_{2h}^2}{4N_{1h}}$, we deduce that $\phi_{5m}^2=\phi_{6m}^2=\frac{N_{2h}}{N_{1h}}$. Thus, two families of kink-shaped solitary solutions of system (1) take the form (see Fig. 4)

$$u_5(x,t)=\pm\sqrt{\frac{N_{2h}}{N_{1h}}}\tanh\left(\sqrt{-\frac{N_{2h}}{2}}\left(k\left(x-v_0t\right)-\xi_0\right)\right)\exp\left(i\left(-\lambda x+\mu t+\theta_0\right)\right). \tag{32}$$

The distinction between the dispersive concatenation model and the RKL equation does not lie not in the exact replication of results but rather in the comprehensive integration of various dispersion effects and underlying models. While the figures may exhibit similar outcomes, it is crucial to note that the mechanisms driving these results differ significantly.

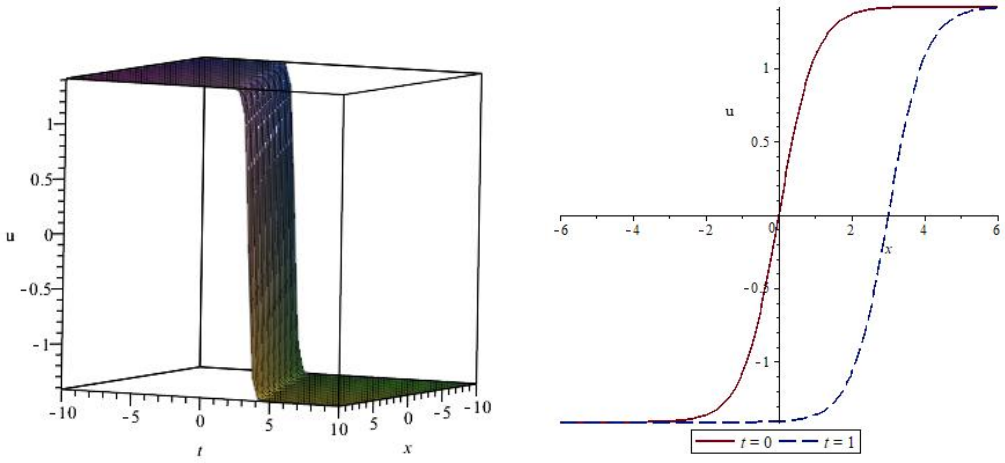

(a) (b)

Fig. 4. The graphics of a kink-shaped solitary solution given by Eq. (32) at $N_{1h}-1$, $N_{2h}=-2$, $v_0=3$, $K=1$, and $\xi_0=0$: (a) real 3D surface; (b) real 2D surface.

The dispersive concatenation model amalgamates three well-known models, each contributing distinct dispersive effects: third-order dispersion, fourth-order dispersion, and fifth-order dispersive effects stemming from the SHE, the LPD model, and the dispersive NLSE, respectively. This integration offers a more nuanced representation of the underlying physical processes.

Conversely, the RKL equation primarily addresses third-order dispersion and may not capture the higher-order dispersion effects in the dispersive concatenation model. While some similarities in the results may exist, the underlying physics and the comprehensive consideration of dispersion effects in the dispersive concatenation model distinguish it from the RKL equation.

3. Conclusions

This paper carried out a comprehensive analysis of the dispersive concatenation model from the bifurcation analysis perspective. The dynamical system yielded the phase portraits of the model. This led to the soliton solutions of the model. These results thus give a fresher and a different perspective to the model. These interesting results are new and are being reported here for the first time. The results are very prospective toward future efforts with the same model. A natural extension of this study would be to look at the dispersive concatenation model with the power-law of SPM and carry out its bifurcation analysis. Later, the model would be studied from various perspectives, such as carrying out its numerical analysis with the aid of Laplace-Adomian decomposition, addressing it with differential group delay, and eventually, for dispersion-flattened fibers. Such results would be sequentially disseminated after aligning them with the pre-existing ones [13-20].

References

1. Tang, L., Biswas, A., Yıldırım, Y., & Alghamdi, A. A. (2023). Bifurcation analysis and optical solitons for the concatenation model. *Physics Letters A*, *480*, 128943.
2. Tang, L. (2022). Bifurcations and dispersive optical solitons for cubic–quartic nonlinear Lakshmanan–Porsezian–Daniel equation in polarization-preserving fibers. *Optik* , *270* , 170000.
3. Li, J.B., Dai, H.H. (2007). *On the study of singular nonlinear traveling wave equations: dynamical system approach*. Science Press.
4. Li, J.B. (2013). *Singular nonlinear traveling wave equations: bifurcation and exact solutions*. Science Press.
5. Tang, L. (2022). Bifurcation analysis and multiple solitons in birefringent fibers with coupled Schrödinger-Hirota equation. *Chaos, Solitons & Fractals*, *161*, 112383.
6. Tang, L. (2022). Bifurcations and dispersive optical solitons for nonlinear Schrödinger–Hirota equation в DWDM networks. *Optik* , *262* , 169276.
7. Tang, L. (2023). Bifurcation studies, chaotic pattern, фаза діаграми і множинні оптичні solitons для (2+ 1)-dimensional stochastic coupled nonlinear Schrödinger система з multiplicative white noise via Itô calculus. *Results in Physics* , *52* , 106765.
8. Ankiewicz, A., & Akhmediev, N. (2014). Higher-order integrable evolution equation and its soliton solutions. *Physics Letters A*, *378*(4), 358-361.
9. Ankiewicz, A., Wang, Y., Wabnitz, S., & Akhmediev, N. (2014). Extended nonlinear Schrödinger equation with higher-order odd and even terms and its rogue wave solutions. *Physical Review E*, *89*(1), 012907.
10. Belyaeva, TL, & Serkin, VN (2012). Wave-particle duality of solitons and solitonic analog of the Ramsauer-Townsend effect. *The European Physical Journal D* , *66* , 1-9.
11. N. A. Kudryashov, NA, Biswas, A., Borodina, AG, Yildirim, Y., & Alshehri, HM (2023). Painlevé analysis and optical solitons для зробленого моделі. *Optik* , *272* , 170255.
12. Triki, H., Sun, Y., Zhou, Q., Biswas, A., Yıldırım, Y., & Alshehri, HM (2022). Тварні кутові pulses and moving fronts in optical medium with high-order dispersive and nonlinear effects. *Chaos, Solitons & Fractals* , *164* , 112622.
13. Wang, M. Y. (2022). Optical solitons with perturbed complex Ginzburg–Landau equation in Kerr and cubic–quintic–septic nonlinearity. *Results in Physics*, *33*, 105077.

14. Wazwaz, A. M., & Mehanna, M. (2021). Higher-order Sasa–Satsuma equation: Bright and dark optical solitons. *Optik*, *243*, 167421.
15. Yıldırım, Y. (2021). Optical solitons with Biswas–Arshed equation by F-expansion method. *Optik* , *227* , 165788.
16. Zhou, Q. (2022).Influence of parameters of optical fibers on optical soliton interactions. *Chinese Physics Letters*. *39*(1), 010501.
17. Jawad, A. J. M., & Abu-AlShaeer, M. J. (2023). Highly dispersive optical solitons with cubic law and cubic-quinticseptic law nonlinearities by two methods. *Al-Rafidain J. Eng. Sci.*, *1*(1), 1-8.
18. Jihad, N., & Abd Almuhsan, M. (2023). Evaluation of impairment mitigations for optical fiber communications using dispersion compensation techniques. *Al-Rafidain J. Eng. Sci*, *1*(1), 81-92.
19. Jawad, A., & Biswas, A. (2024). Solutions of resonant nonlinear Schrödinger's equation with exotic non-Kerr law nonlinearities. *Al-Rafidain J. Eng. Sci.*, *2*(1), 43-50.
20. González-Gaxiola, O., Biswas, A., Yildirim, Y., & Alshehri, H. M. (2022). Highly dispersive optical solitons in birefringent fibres with non-local form of nonlinear refractive index: Laplace–Adomian decomposition. *Ukr. J. Phys. Opt.*, *23*(2), 68-76.
21. Tang, L., Biswas, A., Yıldırım, Y., Aphane, M., & Alghamdi, A. A. (2024). Bifurcation analysis and optical soliton perturbation with Radhakrishnan--Kundu--Lakshmanan equation. *Proceedings of the Estonian Academy of Sciences*, *73*(1).
22. Tang, L., Biswas, A., Yildirim, Y., & Asiri, A. (2023). Bifurcation Analysis and Chaotic Behavior of the Concatenation Model with Power-Law Nonlinearity. *Contemporary Mathematics*, 1014-1025.
23. Tang, L. (2023). Phase portraits and multiple optical solitons perturbation in optical fibers with the nonlinear Fokas–Lenells equation. *Journal of Optics*, *52*(4), 2214-2223.
24. Tang, L. (2023). Bifurcations and optical solitons for the coupled nonlinear Schrödinger equation in optical fiber Bragg gratings. *Journal of Optics*, *52*(3), 1388-1398.
25. Tang, L. (2024). Dynamical behavior and multiple optical solitons for the fractional Ginzburg–Landau equation with β-derivative in optical fibers. *Optical and Quantum Electronics*, *56*(2), 175.
26. Tang, L. (2024). Optical solitons perturbation and traveling wave solutions in magneto-optic waveguides with the generalized stochastic Schrödinger–Hirota equation. *Optical and Quantum Electronics*, *56*(5), 1-15.

Lu Tang, Yakup Yildirim, Anwar Jaafar Mohamad Jawad, Anjan Biswas, & Ali Saleh Alshomrani. (2024). Bifurcation Analysis and Optical Solitons for the Dispersive Concatenation Model. *Ukrainian Journal of Physical Optics*, *25*(3), 03031 – 03039. doi: 10.3116/16091833/Ukr.J.Phys.Opt.2024.03031

Анотація. *У цій роботі проведено біфуркаційний аналіз дисперсійної моделі конкатенації з законом Керра фазової самомодуляції. Спочатку формулюється динамічна система і аналізуються фазово-площинні портрети. Після цього з аналізу відновлюються відповідні розв'язки солітонів.*

Ключові слова*: біфуркаціний аналіз, оптичні солітони, дисперсійна модель конкатенації*